

# Wireline Equalization using Pulse-Width Modulation

Jan-Rutger (J.H.R.) Schrader, Eric A.M. Klumperink, Jan L. Visschers<sup>1</sup>, and Bram Nauta

CTIT Research Institute, IC Design Group, University of Twente,

P.O. Box 217, 7500AE Enschede, The Netherlands

<sup>1</sup>National Institute for Nuclear Physics and High Energy Physics (NIKHEF),

P.O. Box 41882, 1009DB Amsterdam, The Netherlands

E-mail: j.h.r.schrader@utwente.nl

**Abstract**—High-speed data links over copper cables can be effectively equalized using pulse-width modulation (PWM) pre-emphasis. This provides an alternative to the usual 2-tap FIR filters. The use of PWM pre-emphasis allows a channel loss at the Nyquist frequency of  $\sim 30$ dB, compared to  $\sim 20$ dB for a 2-tap symbol-spaced FIR filter. The use of PWM fits well with future high-speed low-voltage CMOS processes. The filter has only one ‘knob’, which is the duty-cycle. This makes convergence of an algorithm for automatic adaptation straightforward. Spectral analysis illustrates that, compared to a 2-tap FIR filter, the steeper PWM filter transfer function fits better to the copper channel. This applies to both half-symbol-spaced and symbol-spaced 2-tap FIR filters. Circuits for implementation are as straightforward as for FIR pre-emphasis. In this paper new measurements are presented for a previous transmitter chip, and a new high-swing transmitter chip is presented. Both coaxial and differential cables are used for the tests. A bit rate of 5 Gb/s (2-PAM) was achieved with all cable assemblies, over a cable length of up to 130 m. Measured BER at this speed is  $<10^{-12}$ .

## I. INTRODUCTION

High-speed data links over short distances are used extensively, for example in datacenters. At speeds in the order of 10 Gb/s, optical links require expensive optical components and driver circuitry, while copper cables can be more economical. With an interconnect length in the order of 10-100 m, good quality copper cables provide a high bandwidth, and either coaxial or differential cables can be used. However, cable losses decrease the receiver eye opening and limit the bit rate at which data can still be reliably detected at the receiver side. Fig. 1 shows the simulated response of a 25 m RG-58CU coaxial cable to a 5 Gb/s 2-PAM signal. The model that was used for the time domain cable simulations is explained in [1],[2]. Clearly this response is severely distorted by ISI.

To compensate for channel losses, transmitter pre-emphasis or receiver equalization can be applied [3-7]. Receiver equalization typically involves several analog blocks which impose speed, accuracy and noise requirements. On the other hand, transmitter pre-emphasis allows the use of a simple receiver that only needs to sample binary values [7]. Pre-emphasis methods found in the literature are commonly based on symbol-spaced FIR (SSF) filtering [3]-[7].

The PWM pre-emphasis (PWM-PE) technique was first used by the authors’ group to equalize on-chip wires [8],[9]. After that, we showed PWM-PE to be very effective

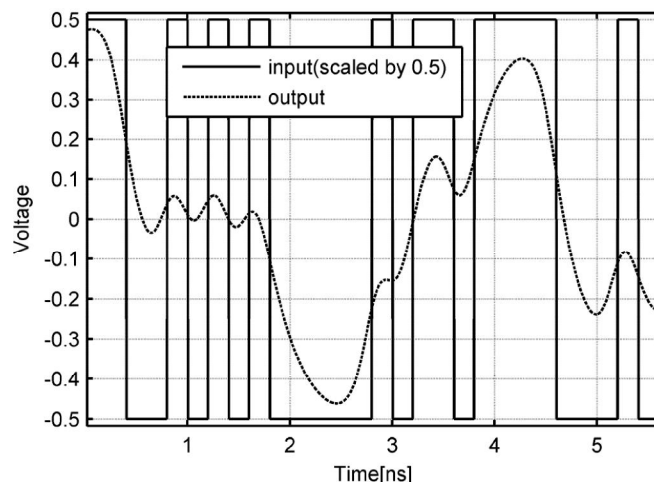


Fig. 1. Simulated response of 25 m RG-58CU coaxial cable to 5 Gb/s data.

for equalization of copper cables [10]. Measurements were made with a  $0.13\mu\text{m}$  PWM-PE transmitter chip. A BER of  $<10^{-12}$  was achieved at 5 Gb/s, with a channel loss of 33dB at 2.5GHz. A 25 m low-end, low-cost RG-58CU coaxial cable was used. Next, in [1], the PWM-PE filter transfer function, the ISI dependence on bit rate, and the timing sensitivity were analyzed.

This paper discusses the PWM pre-emphasis technique and summarizes the results of the first test chip. Furthermore, a new chip with larger output swing and reduced power consumption is presented. New measurements of both chips are given with four different cable types. Section II introduces PWM-PE and outlines the differences with FIR pre-emphasis filtering. It provides a theoretical comparison with 2-tap FIR filters. It is shown that a higher cable attenuation can be handled with PWM-PE. In section III, the frequency-dependent loss of copper cables is analyzed, both for differential and coaxial cables. Section IV and V present the measured performance of the prototypes. Finally, conclusions are drawn in section VI.

## II. PULSE-WIDTH MODULATION PRE-EMPHASIS

PWM-PE exploits the timing resolution available in modern CMOS processes. It does not tune the pulse amplitude (tap weights) to adjust the filter to the cable, like a FIR filter. This will be beneficial in future CMOS generations, because of ever increasing switching speeds,

whereas voltage headroom is becoming lower. The filter can be implemented on a low area and with a low power consumption because it only involves an adjustable duty-cycle.

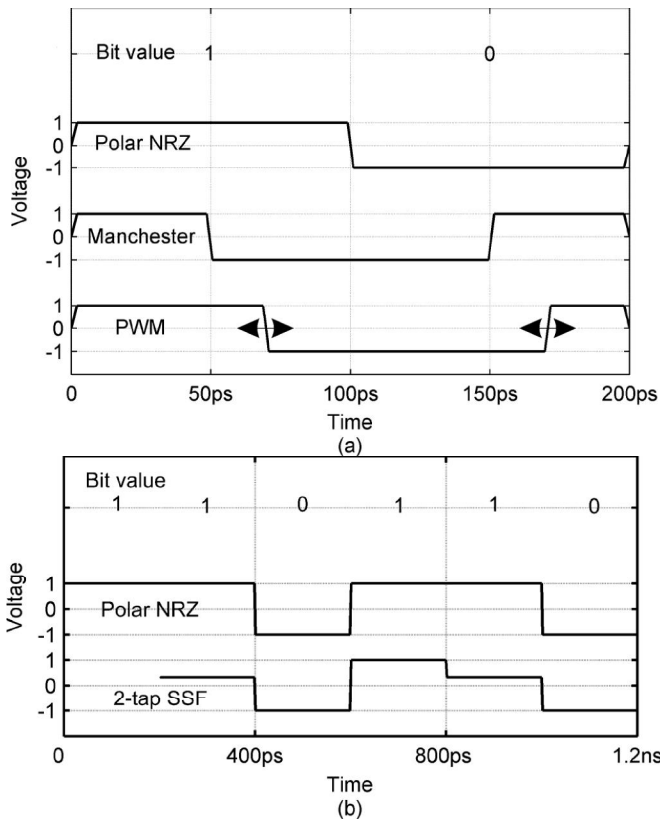


Fig. 2. Output signals for PE transmitters,  $T_s=200$ ps. (a). PWM pre-emphasis. (b). 2-tap SSF pre-emphasis.

In Fig. 2(a), the output voltage waveform for the PWM-PE filter is shown. The output is normalized to a +/- 1V supply. We assume that the modulation scheme is 2-level Pulse Amplitude Modulation (PAM). The PWM pulse shape resembles a Manchester-coded signal, but where the Manchester duty-cycle is fixed at 50%, the PWM signal instead has a tunable duty-cycle. A duty-cycle of 100% corresponds to transmission of a normal polar NRZ data signal without pre-emphasis, and 50% to transmission of a Manchester coded data signal (maximum pre-emphasis setting). The optimum duty-cycle is somewhere in between, depending on the channel characteristics. In comparison, Fig. 2(b) shows the output of a 2-tap symbol-spaced FIR (SSF) transmitter, again normalized to a +/- 1V supply. Both types of PE have only one ‘knob’, making a coefficient finding algorithm converge quickly and straightforwardly.

For a quick insight into PWM-PE filtering, the simulated time domain response of a 25 m low-cost, low-end, standard RG-58CU cable to PWM pulses with several duty-cycles and  $T_s=200$ ps is shown in Fig. 3. This cable is used later in the experiments. The time domain cable model includes both skin-effect and dielectric losses, and is explained in [1],[2].

The sample moment  $t_s$  is shown with a triangle, and the ISI contributions are shown with circles. Note that for the duty-cycle setting of 55%, the cable output pulse becomes much narrower than the response to a plain polar NRZ pulse (100%). This reduces the ISI contributions significantly. It is seen that an optimum setting can be found at which the ISI is minimized. Second, note that the optimum duty-cycle is near - but not equal to - 50%. As a comparison, in Fig. 4 the response of the channel to 2-tap SSF pulses is shown. (Parameter  $r$  is described below.) It can be seen that PWM-PE is capable of narrowing the channel pulse response, similar to FIR pre-emphasis.

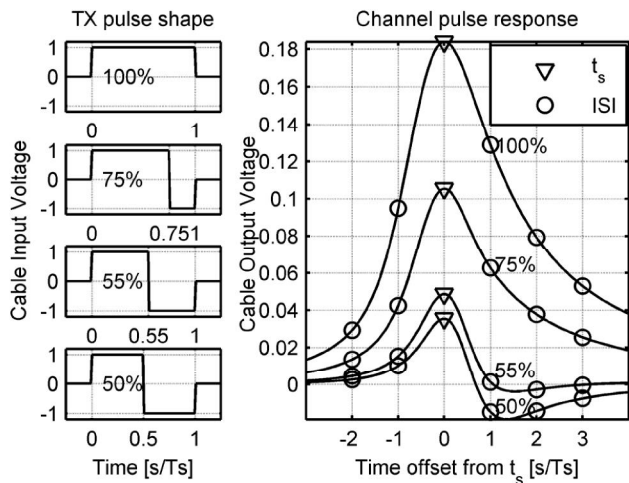


Fig. 3. TX pulse shapes ( $T_s=200$ ps) of PWM-PE filter with varying duty-cycles and simulated responses of 25 m RG-58CU cable.

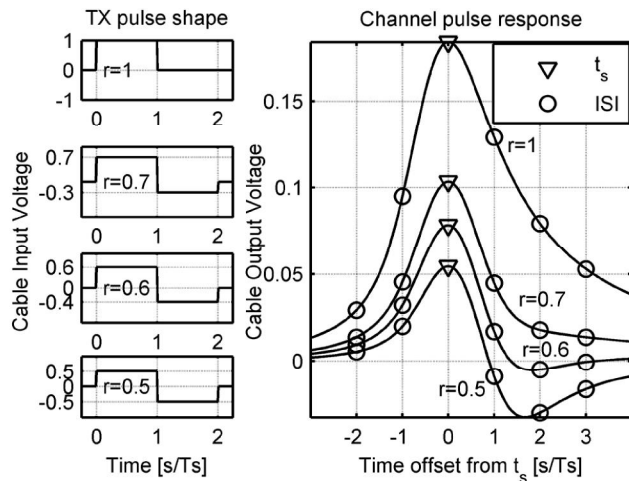


Fig. 4. TX pulse shapes ( $T_s=200$ ps) of SSF-PE filter with varying  $r$  parameter and simulated responses of 25 m RG-58CU cable.

In practice, PWM duty-cycle  $d$  can be adapted to the channel automatically using return channel communication and a control algorithm. The need for a return channel is a disadvantage compared to receiver equalization, but it is common among all pre-emphasis approaches. A sign-sign block least mean squares (LMS) algorithm can be used as shown in [11]. Such a control algorithm could also

compensate for temperature and channel variations. Convergence of the LMS algorithm for the single-coefficient PWM-PE filter is more straightforward than it would be for a filter with multiple coefficients.

PWM-PE achieves more high-frequency boost than 2-tap SSF and half-symbol-spaced FIR filters. This results in a better loss compensation for copper cables. Here, “loss compensation” is defined as cable loss at the Nyquist frequency at which transmission with BER  $<10^{-12}$  is still possible. For a signaling rate of 5 Gb/s, the Nyquist frequency is 2.5GHz. The transfer functions of the PWM and 2-tap SSF filters are given below. For ease of comparison, the TX outputs of all filters are normalized to  $\pm 1V$ , as illustrated in Fig. 2. The modulus of the PWM filter transfer function  $|H_{pwm}(f)|$ , calculated in [1], can be simplified to

$$|H_{pwm}(f)| = \sqrt{2 \frac{\cos(\omega(d-1)T_s) + \cos(\omega d T_s) - 2}{\cos(\omega T_s) - 1} - 1}, \quad (1)$$

where  $d$  denotes the duty-cycle ( $0.5 < d < 1$  fits best to copper cables) and  $T_s$  denotes the symbol duration. This transfer function is illustrated in Fig. 5(a) for several values of  $d$ . It can be seen from this figure that a duty-cycle closer to 50% results in a steeper transfer function. Changing the duty-cycle from 100% toward 50% attenuates the low-frequency components of the pulse spectrum as compared to the spectrum of a polar NRZ pulse. The result is pre-emphasis filtering.

The function  $|H_{pwm}(f)|$  will now be compared to the modulus of the transfer function  $|H_{fir}(f)|$  of the 2-tap SSF. This function, calculated in [1], can be simplified to

$$|H_{fir}(f)| = \sqrt{(r^2 - r) \frac{\cos(2\omega T_s) - 1}{\cos(\omega T_s) - 1} + 1}, \quad (2)$$

with one coefficient  $r$ , chosen from the range  $\{0.5..1\}$ , that completely controls the shape of the normalized filter transfer function. This function is illustrated in Fig. 5(b) for several values of  $r$ . The closer  $r$  is to 0.5, the more low-frequency attenuation the filter exhibits. Comparing it to the PWM transfer in Fig. 5(a), it can be seen that in the low frequency (LF) range the PWM-PE filter behaves like the 2-tap SSF filter, however in the high frequency (HF) range the PWM-PE filter offers a higher attenuation. Note that both filters leave the amplitude of the fastest data transitions ( $'101010'$ ) unchanged. This is precisely what a pre-emphasis filter should do. Ideally, it attenuates all frequencies below Nyquist and leaves the fastest transitions untouched. That fits best to the cable, which has an attenuation that increases monotonically with frequency, as is shown in section III. The cable loss at the Nyquist frequency therefore roughly determines the eye height at the cable output. This eye height is approximately the same for both filters up to  $\sim 20$ dB cable loss at the Nyquist frequency. After that, the eye of the 2-tap

SSF closes and PWM-PE still has an open eye, up to  $\sim 30$ dB.

Finally, one could ask whether PWM filtering boils down to the same thing as 2-tap half-symbol-spaced FIR filtering. This is not the case, because whereas the PWM filter attenuates only the signals below the Nyquist frequency, a 2-tap half-symbol-spaced FIR filter attenuates the signals at the Nyquist frequency as well. The 2-tap half-symbol-spaced filter has a two times wider frequency response than its 2-tap SSF brother. However, as a result of that, the transfer function is stretched out and is not as steep as that of the PWM-PE filter in the frequency range from zero to Nyquist, resulting in a lower loss compensation. Half-symbol-spaced FIR filters are sometimes used at the receiver side [3].

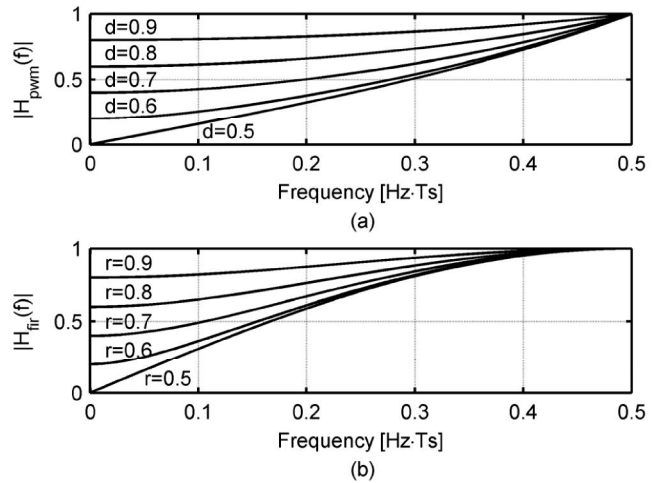


Fig. 5. Calculated normalized magnitude of filter transfer. (a). PWM-PE filter. (b). 2-tap SSF-PE filter.

### III. Cables

We use two types of copper cables in our measurements: coaxial and differential cables. Our goal with these cables is to achieve a BER figure of  $<10^{-12}$ , using a PWM pre-emphasis transmitter and a PAM-2 receiver without equalizer. The cables have to meet certain requirements, which are the same as for 2-tap FIR pre-emphasis. First, that the cable is manufactured with a characteristic impedance that is continuous and independent of position along the cable. Second, that the cable is characteristically terminated to avoid reflections. PWM-PE alone is unable to compensate for a channel with reflections, because it offers only one degree of freedom. Third and finally, that the cable loss at the Nyquist frequency is not larger than 30dB. This is the maximum achievable loss compensation for PWM-PE, as will be shown later experimentally.

The characteristic impedance of a cable is not very easy to control. It is a function of, among other things, the distance between the conductors. In good quality cables, designed for high-bandwidth interconnects, this distance does not vary much with position, not even with several bends in the cable. In most coaxial cables this is the case. For low-quality differential (twisted-pair) cables, the distance between the conductors may vary. For our experiments, we have selected a high-quality differential cable designed for the 10GBASE-CX4 standard. In a low-quality twisted-pair cable like

CAT-5, the distance is not well controlled, resulting in a higher-order transfer function which requires a higher order equalizer.

The cable frequency transfer function  $H_c(f)$  (excluding propagation delay) can be well approximated by [12]-[14]:

$$H_c(f) = e^{-\sqrt{j2\pi f\tau_1} - 2\pi f\tau_2} \quad (3)$$

The time constants  $\tau_1$  and  $\tau_2$  quantify the two loss effects in the copper cable. These are the skin effect ( $\tau_1$ ) and the dielectric polarization/relaxation ( $\tau_2$ ). These effects cause dispersion and frequency dependent attenuation. The time constants are dependent on the length of the cable, the radius of the conductors and the distance between them, the conductivity and magnetic permeability of the conductors, and the electric permittivity and loss tangent of the dielectric. The loss tangent is dependent on the material of the dielectric, and the conductance is dependent on the conductor type. The conductor can be for example solid copper, or woven copper. A calculation of the time constants is given in [2].

To be able to assess the PWM-PE performance under several channel conditions, four different cable assemblies were used for the measurements:

- (a) - 25 m RG-58CU (coaxial),
- (b) - 130 m Aircom+ (coaxial),
- (c) - 80 m Aircell7 (coaxial),
- (d) - 15 m 10GBASE-CX4 (24AWG shielded differential).

TABLE I  
COMPARISON OF CABLE PARAMETERS

Cable type	Inner conductor diameter / type	Outer diameter	Dielectric type	Loss/100m @2.5GHz
(a)	0.9 mm, woven	5,1 mm	PE	124dB
(b)	2.7 mm, solid	10.3 mm	Air	23dB
(c)	1,85 mm, woven	7.3 mm	Foam	37dB
(d)	0.5mm (24AWG)	10mm	Foam	127dB

Table I shows a summary of the cable parameters. Cable (a) is a low-cost, low-end, standard coaxial cable with polyethylene dielectric. Cable (b) is a more expensive coaxial cable with low-loss air dielectric, designed for frequencies up to 10GHz. It is however rather rigid and has a large diameter. Cable (c) has a foam dielectric and an inner conductor of woven copper. Therefore it is much more flexible and thinner than (b), while still offering a relatively low dielectric loss. Finally cable (d), which is the most expensive, contains 8 shielded differential pairs and is designed for a bit rate of 3.125 Gb/s per pair using 2-tap SSF at the transmitter. All coaxial cables have a characteristic impedance of 50Ω and (d) has a differential characteristic impedance of 100Ω. The lengths of the coaxial cables are chosen in such a way that the equalizer can be tested at the

highest speed and maximum loss compensation that it can handle. Cable (d) was not available longer than 15 m.

The measured and modeled magnitudes of the transfer function  $S_{21}$  for the cables are shown in Fig. 6. The modeled contribution of conductor losses and dielectric losses is shown separately. Cable (b) has the highest ratio of skin loss to dielectric loss, because of its air dielectric. Overall, agreement between model and measurements is good as far as the modulus of the transfer function is concerned. Up to 4GHz, the model is accurate to <2dB.

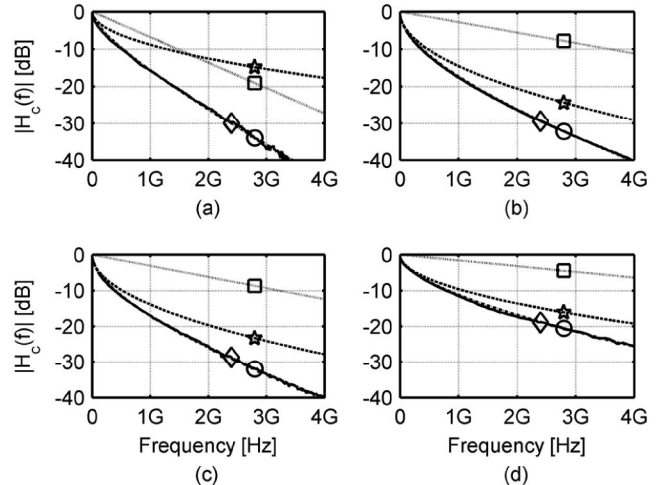


Fig. 6. Measured and modeled cable transfer functions. Diamond: measured  $S_{21}$ . Star: skin loss, model. Square: dielectric loss, model. Circle: total loss, model. (a). 25 m RG-58CU. (b). 130 m Aircom+. (c). 80 m Aircell7. (d). 15 m 10GBASE-CX4 24AWG. (Measured:  $S_{dd21}$ .)

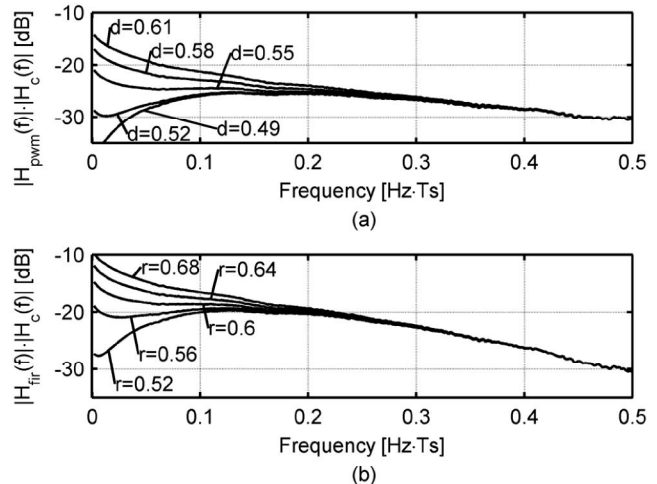


Fig. 7. Equalized transfer of 25 m RG-58CU. (a). PWM. (b). 2-tap SSF.

Next, we will calculate the equalized channel transfer function for the 2-tap symbol-spaced FIR filter and the PWM filter. A theoretical first-order channel can be perfectly equalized with PWM pre-emphasis as calculated in [9]. A cable does not have a first order transfer function but still can be equalized with PWM pre-emphasis. The equalized transfer function is calculated by taking the measured cable transfer of 25 m RG-58CU and multiplying it with the calculated theoretical transfer of the pre-emphasis filters. A bit length of  $T_s=200ps$  is chosen. The results are shown in Fig. 7. The channel response

for PWM pre-emphasis is flat to within 5dB, while the FIR response is only flat to within 10dB. PWM-PE clearly outperforms FIR-PE. For shorter cable lengths the responses become flatter. Half-symbol spaced 2-tap FIR is not shown here to save space, but it is flat only to within 8dB.

#### IV. CHIP 1: DESIGN AND MEASUREMENTS

In this section and the next, the two chip designs and their measured performance are presented. Both chips are designed in current-mode logic (CML) to provide maximum supply noise rejection and minimum supply noise injection and to keep timing noise as low as possible. Bandwidth limitations in the circuitry do not pose a problem because they will just become part of the total channel transfer function that needs to be compensated by the pre-emphasis. A difference between up- and down- slew rate would have a negative effect on the fit of the pre-emphasis to the channel. The use of differential CML guarantees symmetrical up- and down- slew rates. An advantage over FIR pre-emphasis is that non-linear (symmetrical) slewing effects do not affect the equalizer's fit to the channel because only two signal levels are used.

The first chip was designed in a 0.13 $\mu$ m technology, and the second in a 90nm technology. In this section, we will describe the 0.13 $\mu$ m chip and give measurement results. In the next section, we will describe the 90nm chip and give measurement results.

##### A. Circuit Overview

The operation principle of chip 1 is shown in Fig. 8(a). The data is XOR'ed with a pulse-width modulated clock in order to provide pre-emphasized data. The PWM clock is generated using an OR gate and a delay circuit. The timing of the signals is illustrated in Fig. 8(b). A more detailed description of the circuit is given in [1].

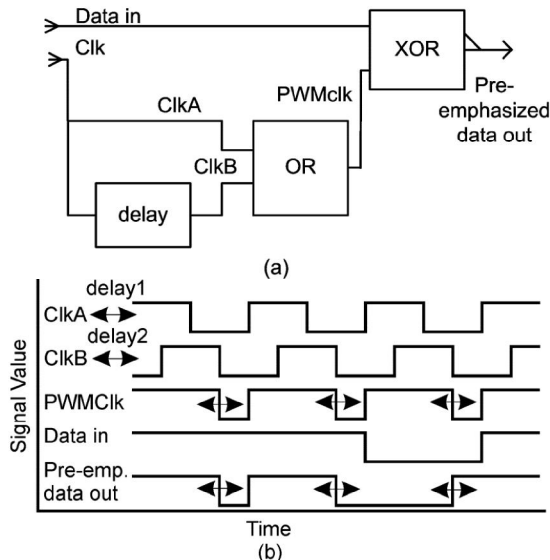


Fig. 8. (a). Circuit operation principle for chip 1. (b). Signals used in generating PWM signal.

##### B. Line Driver

The line driver of chip 1 consists of three stages (Fig. 9). The final stage has a 50 $\Omega$  on-chip termination resistance and a tail current of 24mA. This results in a nominal single-ended output swing of 600mV<sub>p-p</sub> in a 50 $\Omega$  cable. This corresponds to a differential voltage of 1.2V<sub>p-p</sub>. The line driver power is 42mW from 1.2V.

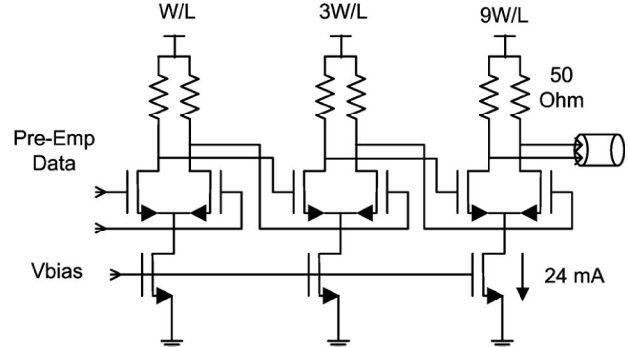


Fig. 9. Three-stage differential line driver of chip 1.

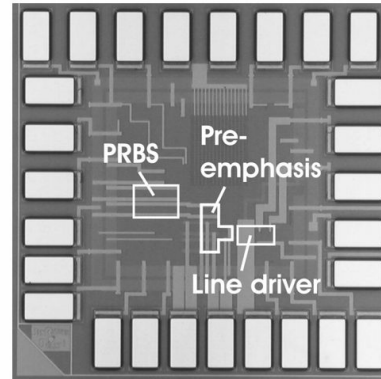


Fig 10. Microphotograph of chip 1, 1x1 mm<sup>2</sup>.

##### C. Measurements

A microphotograph of the first chip is shown in Fig. 10. It measures 1x1 mm<sup>2</sup>, and has an active area of approximately 150x150  $\mu$ m<sup>2</sup>. All chip I/Os have on-chip 50 $\Omega$  termination and are ESD protected.

To evaluate the performance of the prototype chips, eye diagrams and BER tests were made. All measurements were made using the four cable assemblies described above. For chip 1, the DC voltages/currents, including the power supply, were connected to a PCB by wirebonds, and the high speed in-/outputs were probed. A 50 $\Omega$  differential probe with 4 pins was used: ground-signal-signal-ground. If the high-speed data outputs would be connected via a PCB, there might be an impedance change from the PCB to the cable, causing reflections. However, these reflections would be largely absorbed by the transmitter termination resistors.

##### Effect of Adjustments in PWM Duty-Cycle

In Figs. 11(a), (c) and (e), the effect of adjusting the PWM duty-cycle on the transmitter output can be seen. The left- and right edges in the eye diagrams correspond to the

symbol edges. In Figs. 11(b), (d) and (f), the responses of a 10-m RG-58CU cable to the pre-emphasized data stream with different pre-emphasis duty-cycles are shown. It can be seen that there is an optimum duty-cycle [Figs. 11(c) and (d)]. Under-emphasis is shown in Figs. 11(a) and (b) and over-emphasis in Figs. 11(e) and (f). Note that the time scale is the same in all subfigures. The PWM pre-emphasis leaves the fastest data pattern ('101010') unchanged while it attenuates the data patterns with less transitions per second.

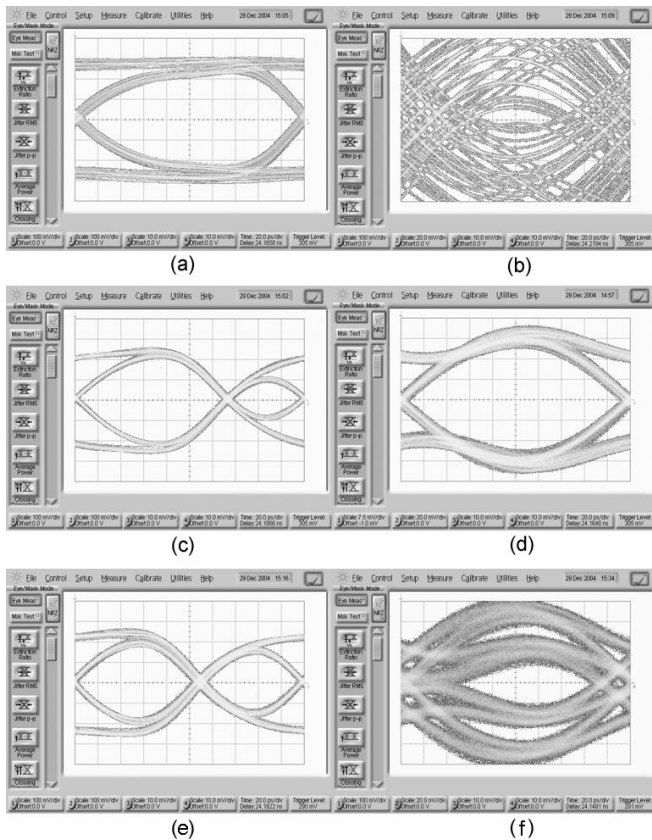


Fig. 11. Measured eye-diagrams for transmitter output and cable output (10 m RG-58CU) at 5 Gb/s. Horizontal axis = 20ps/div, vertical axis is 100mV/div. for (a), (c) and (e), and 20mV/div for (b), (d) and (f). (a). TX, no pre-emphasis (100%). (b). RX, no pre-emphasis (100%). (c). TX, optimum pre-emphasis (66%). (d). RX, optimum pre-emphasis (66%). (e). TX, strong pre-emphasis (55%). (f). RX, strong pre-emphasis (55%).

### Eye Diagrams at Max. Loss Compensation

The requirement for all measurements is to achieve a BER of  $<10^{-12}$ . The cable lengths are chosen such that this BER figure can be achieved at a bit rate of 5 Gb/s, the highest speed achievable with the TX circuitry. The channel loss at the Nyquist frequency can then be taken as a figure-of-merit for the equalizer. We call this the 'loss compensation' of the equalizer. In Figs. 12(a)-(d), measured eye diagrams of the cable outputs at 5 Gb/s are shown. All four cable types, described in section III, are shown. Figs. (a)-(c) are for the coaxial cables and Fig. (d) is for the differential cable. For the coaxial cables, one of the two transmitter outputs was used while the other was terminated with a 50Ω dummy. For

the differential cable, both transmitter outputs were used. The oscilloscope input is single-ended. Therefore, the eye-diagram shown in Fig. 12(d) was measured at the output of the differential limiting amplifier. For cables (a)-(c), the loss at 2.5GHz is ~30dB. For cable (d), the loss at 2.5GHz is 19dB. The total channel loss is a few dB more than the cable loss alone, because of additional losses from probes, short wire, bias tee and connectors. Using an external pattern generator and tester, the BER was tested with all cable assemblies at 5 Gb/s and is  $<10^{-12}$ .

At a channel loss of >30dB, the small cable output amplitude imposes a high demand on receiver sensitivity. For the BER measurements a limiting amplifier was used with a 1mV input offset. Using the fully differential transmitter capabilities with cable (d) offers the advantage of a 6dB higher (differential) swing while also rejecting common mode noise.

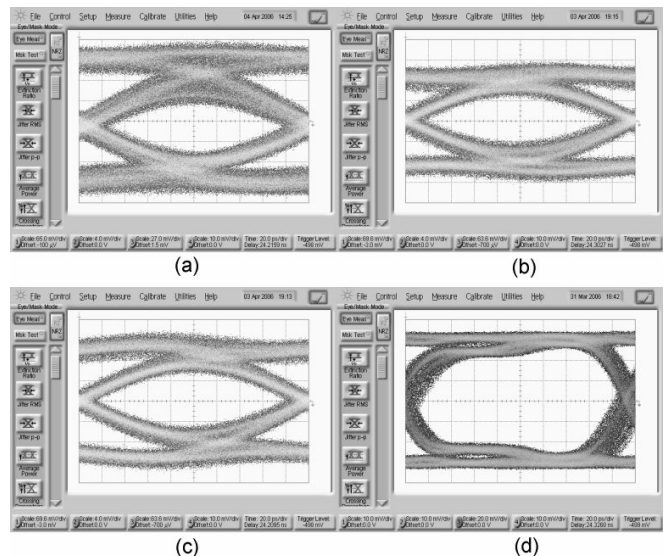


Fig. 12. Measured output eyes of chip 1 at 5 Gb/s and BER  $<10^{-12}$ . Horizontal axis = 20ps/div, vertical axis is 4mV/div. for Figs. (a)-(c) and 20mV/div. for Fig. (d). (a). 25 m RG-58CU. (b). 130 m Aircom+. (c). 80 m Aircell7. (d). 15 m 10GBASE-CX4 24AWG after differential limiting amplifier.

TABLE II  
PRE-EMPHASIS COMPARISON WITH OTHER WORK

Ref.	R	Loss	Process	Type
[3]	8 Gb/s	~10dB	0.3μm	2-tap FIR
[4]	4 Gb/s	~10dB	0.25μm	2-tap FIR
[5] TX only	5 Gb/s	18dB	0.13μm	2-tap FIR
[6] TX only	3.125 Gb/s	30dB	0.11μm	5-tap FIR
this work	5 Gb/s	33dB	0.13μm	PWM

From [5,6] only the transmitter pre-emphasis is taken into account (not the receiver equalizer). Ref. [3] describes a 4-PAM transmitter.

In table II, a comparison with other published work is given. In [5], a combination of pre-emphasis and post-equalization has yielded 27dB (18dB+9dB) loss

compensation at a signaling rate of 5 Gb/s. None of the pre-emphasis filters that use 2 taps [3]-[5] offer more than 18dB loss compensation. A 5-tap FIR filter in [6] reached 30dB but only at 3.125 Gb/s. More taps can offer higher loss compensation but at the expense of increasing complexity, possibly causing accuracy and speed problems. Furthermore, algorithm convergence for automatically finding the optimum equalizer coefficients is more troublesome than for an equalizer with only one ‘knob’. The PWM-PE filter presented here offers a record loss compensation (33dB), at a bit rate of 5 Gb/s.

## V. CHIP 2: DESIGN AND MEASUREMENTS

The second chip was designed with the results from the first in mind. The high cable loss results in a low amplitude at the cable output, which can lead to problems at the receiver side. The SNR might be too low, or the received signal amplitude might be below the receiver offset. A usual value for the receiver offset is  $\sim 50\text{mV}$ . Therefore, it would be convenient to have a transmitter with a higher output swing.

### A. Line Driver

The line driver circuit of chip 2 extends the line driver of chip 1 by cascading a cascode stage. High-voltage transistors are not needed. This enables a maximum output voltage of 2.5V. The output current is adjustable from 36-74mA, resulting in a 1.8Vp-p single-ended voltage swing in  $50\Omega$  or  $25\Omega$ , the latter in case of an external TX termination resistor. Compared to the first chip, the TX power is almost 10dB larger. This would lead to high power dissipation in an on-chip TX termination resistor, dissipating  $(1.8)^2/50=65\text{mW}$ . The excess heat could pose a problem when many high-speed links are operated in parallel. For that reason the TX termination resistor was left out and the driver is open-drain. It is shown in Fig. 13. The cable needs to be terminated to 2.5V, in order to supply the driver bias current.

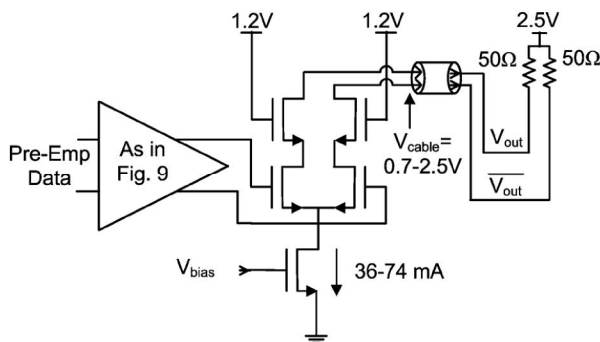


Fig. 13. Line driver of chip 2 with cable and termination.

### B. Duty-cycle tuning circuit

A duty-cycle tuning circuit different from that in chip 1 is chosen, because that one has some disadvantages. It requires adjustment of two voltages, and is not nominally set at 50%, which is convenient for a cable with significant loss. The circuit of chip 2 has a nominal setting of 50% [15]. It outputs

a duty-cycle of 50% at a differential voltage  $V_{dutyP}-V_{dutyN}=0\text{V}$ , and is shown in Fig. 14.

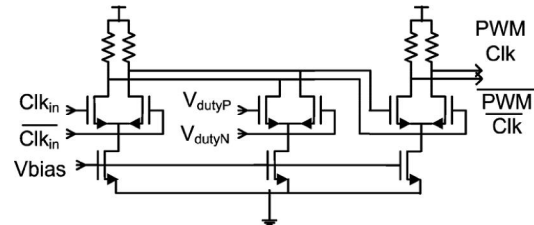


Fig. 14. Duty-cycle tuning circuit of chip 2.

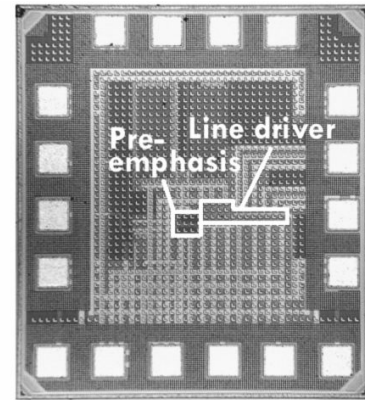


Fig 15. Chip 2 microphotograph,  $1\times 0.9\text{ mm}^2$ .

### C. Measurements

A microphotograph of chip 2 is shown in Fig. 15. The chip measures  $1\times 0.9\text{ mm}^2$ , and has an active area of approximately  $100\times 100\text{ }\mu\text{m}^2$ . Both the DC voltages/currents, including the power supply, and the high speed in-/outputs were connected via probes. Because our oscilloscope is terminated to ground, a bias tee was used at the cable output. This way we could still supply the driver bias current while terminating the cable to ground. The DC input of the bias tee was connected to 1.65V, which is the threshold voltage of the driver output ( $2.5-1.8/2=1.65\text{V}$ ).

The output of the TX at 4 Gb/s is shown in Fig. 16, clearly showing its high swing. In Figs. 17(a)-(d), measured eye diagrams of the cable outputs are shown. The maximum speed achieved with cables (a)-(c) is 3 Gb/s for a BER  $< 1\cdot 10^{-12}$ . The loss of cables (a)-(c) at 1.25GHz is  $\sim 22\text{dB}$ . For the differential cable (d), a speed of 5 Gb/s was achieved. The loss of this cable at 2.5GHz is 19dB. A possible explanation for the difference in loss compensation with chip 1 is the data-dependent noise at the TX output. From Fig. 16, separate lines can be identified. The  $2^7-1$  PRBS pattern repeats after 127 bits. The lines disappear when the PRBS pattern is switched from  $2^7-1$  to  $2^{31}-1$ . We are currently looking into this problem and we are trying to solve it.

The measured eye openings in Figs. 17(a)-(c) are clearly larger than for chip 1, due to the larger TX output swing, even when the 8dB difference in channel loss at the (lower) Nyquist frequency is taken into account.

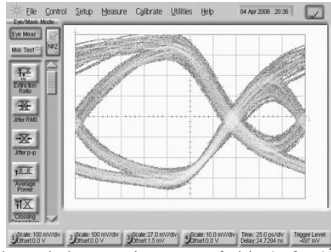


Fig. 16. Single-ended transmitter eye of chip 2, for  $2^7-1$  PRBS pattern at 4 Gb/s. Horizontal axis = 25ps/div., Vertical axis=100mV/div. (10dB att.)

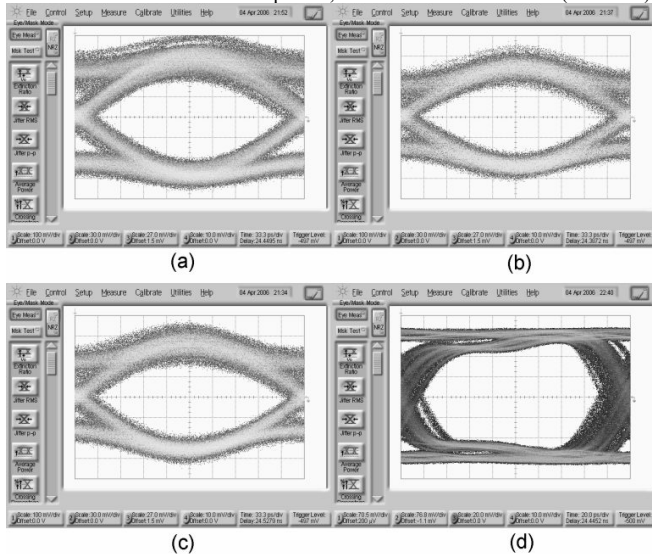


Fig. 17. Measured output eyes of chip 2 at  $BER < 10^{-12}$ . Horizontal axis is 33.3ps/div for Figs. (a)-(c), and 20ps/div. for Fig. (d). Vertical axis is 30mV/div. for Figs (a)-(c), and 20mV/div. for Fig. (d). (a). 25 m RG-58Cu at 3 Gb/s. (b). 130 m Aircom+ at 3 Gb/s. (c). 80 m Aircell7 at 3 Gb/s. (d). 15 m 10GBASE-CX4 24AWG at 5 Gb/s after differential limiting amp.

## VI. CONCLUSIONS

High-speed data links over copper cables can be effectively equalized using pulse-width modulation (PWM) pre-emphasis. This provides an alternative to the usual 2-tap FIR. The use of PWM pre-emphasis allows a channel loss at the Nyquist frequency of  $\sim 30$ dB, compared to  $\sim 20$ dB for a 2-tap symbol-spaced FIR filter. This fits well with future high-speed low-voltage CMOS processes. The PWM duty-cycle determines the shape of the transfer function. Therefore, the filter has only one 'knob'. This makes convergence of an algorithm for automatic adaptation straightforward. Spectral analysis illustrates that, compared to a 2-tap FIR filter, the steeper PWM filter transfer function fits better to the copper channel. The equalized channel transfer function is the flattest for PWM pre-emphasis, compared to both half-symbol-spaced and symbol-spaced 2-tap FIR filters. Circuits for implementation are as straightforward as for FIR pre-emphasis. Two transmitter chips were designed and manufactured as a proof-of-concept. Chip 2 has a higher TX swing than chip 1, to compensate for the high channel loss. The TX termination resistance was left out of chip 2 to keep power dissipation low. Chip 2 however has some data-dependent noise at the TX output. The chips were tested with three types of coaxial

cable and one differential cable. The cable lengths were 25 m, 80 m, 130 m and 15 m, respectively. The loss at 2.5GHz is  $\sim 30$ dB for the three coaxial cables and 19dB for the differential cable. A  $BER < 10^{-12}$  at 5 Gb/s (2-PAM) was achieved with chip 1 for all cable assemblies.

## ACKNOWLEDGMENT

The authors would like to thank Stichting FOM for funding, CERN and Philips for (organizing) chip fabrication, Fujitsu for connectors, D. Schinkel, P. Moreira, G. Cervelli, D.M.W. Leenaerts and H. Verkooijen for help and helpful discussions, W. C. van Etten for the cable model, M. Kuijk for equipment use, and H. de Vries, G. J. M. Wienk, and J. Rövekamp for practical assistance.

## REFERENCES

- [1] J. H. R. Schrader, E. A. M. Klumperink, J. L. Visschers, and B. Nauta, "Pulse-Width Modulation Pre-Emphasis Applied in a Wireline Transmitter, Achieving 33 dB Loss Compensation at 5-Gb/s in 0.13- $\mu$ m CMOS," *IEEE J. Solid-State Circuits*, vol. 41, no. 4, pp. 990–999, Apr. 2006.
- [2] J.H.R. Schrader, E.A.M. Klumperink, J.L. Visschers and B. Nauta, "Data communication in read-out systems: how fast can we go over copper wires?," *Nuclear Instruments and Methods in Physics Research Section A*, vol. 531, no. 1-2, pp. 221-227, Sep. 2004.
- [3] R. Farjad-Rad, C. K. Yang, M. Horowitz, and T. Lee, "A 0.3- $\mu$ m CMOS 8 Gb/s 4-PAM serial link transceiver," *IEEE J. Solid-State Circuits*, vol. 35, no. 5, pp. 757–764, May 2000.
- [4] M. Lee, W. Dally, and P. Chiang, "Low-power area-efficient high-speed I/O circuit techniques," *IEEE J. Solid-State Circuits*, vol. 35, no. 11, pp. 1591–1599, Nov. 2000.
- [5] Y. Kudoh, M. Fukaiishi, and M. Mizuno, "A 0.13- $\mu$ m CMOS 5-Gb/s 10-m 28 AWG cable transceiver with no-feedback-loop continuous-time post-equalizer," *IEEE J. Solid-State Circuits*, vol. 38, no. 5, pp. 741–746, May 2003.
- [6] W. Gai, Y. Hidaka, Y. Koyanagi, J. H. Jiang, H. Osone, and T. Horie, "A 4-channel 3.125 Gb/s/ch CMOS transceiver with 30 dB equalization," in *Symp. VLSI Circuits Dig. Tech. Papers*, Jun. 2004, pp. 138–141.
- [7] W. J. Dally and J. Poulton, "Transmitter equalization for 4 Gb/s signaling," *IEEE Micro*, vol. 17, no. 1, pp. 48-56, Jan.-Feb. 1997.
- [8] D. Schinkel, E. Mensink, E. A. M. Klumperink, A. J. M. van Tuijl and B. Nauta, "A 3Gb/s/ch Transceiver for RC-limited On-Chip Interconnects," in *IEEE Int. Solid-State Circuits Conf. (ISSCC) Dig. Tech. Papers*, Feb. 2005, pp. 386-387.
- [9] D. Schinkel, E. Mensink, E. A. M. Klumperink, A. J. M. van Tuijl, and B. Nauta, "A 3-Gb/s/ch Transceiver for 10-mm Uninterrupted RC-Limited Global On-Chip Interconnects," *IEEE J. Solid-State Circuits*, vol. 41, no.1, pp. 297–306, Jan. 2006.
- [10] J. H. R. Schrader, E. A. M. Klumperink, J. L. Visschers, and B. Nauta, "CMOS transmitter using pulse-width modulation pre-emphasis achieving 33 dB loss compensation at 5-Gb/s," in *Symp. VLSI Circuits Dig. Tech. Papers*, Jun. 2005, pp. 388–391.
- [11] J. T. Stonick, G.-Y. Wei, J. L. Sonntag, and D. K. Weinlader, "An adaptive PAM-4 5-Gb/s backplane transceiver in 0.25  $\mu$ m CMOS," *IEEE J. Solid-State Circuits*, vol. 38, no. 3, pp. 436–443, Mar. 2003.
- [12] F. E. Gardiol, *Lossy Transmission Lines*. Norwood, MA: Artech House, 1987.
- [13] P. Grivet and P. W. Hawkes, *The Physics of Transmission Lines at High and Very High Frequencies*. New York: Academic Press, 1970.
- [14] R.A. Chipman, *Transmission Lines*. New York: McGraw-Hill, 1968.
- [15] P. Westergaard, T.O. Dickson, and S.P. Voinigescu, "A 1.5V 20/30 Gb/s CMOS backplane driver with digital pre-emphasis," in *Proc. IEEE Custom Integrated Circuits Conf. (CICC)*, Oct. 2004, pp. 23–26.